

Scalar vorticity transitions in viscous two-dimensional stagnation flow

Kamen N. Beronov[†] and Shigeo Kida[‡]

[†] *Research Institute for Mathematical Sciences, Kyoto University*

[‡] *Theory and Simulation Center, National Institute for Fusion Science*

1 Introduction

A two-dimensional stagnation point flow $(-Sx, 0, Sz)$ induces constant strain $S > 0$ which can drive stationary or time-dependent self-similar shear layers [1, 2]. The vorticity of such a flow is only along the stretching axis, $(0, 0, \Omega(t, y))$. The cancellation of the nonlinearity in the Navier-Stokes equation produces a linear solution with freely chosen amplitude, $\Omega = (V_\infty/a) \exp(-\frac{1}{2}(y/a)^2)$, where the self-similar profile width $a(t) = 1/\sqrt{\delta^{-2} + e^{-St}(a(0)^{-2} - \delta^{-2})}$ tends to the equilibrium layer thickness $\delta = \sqrt{\nu/S}$. Both the viscosity $\nu > 0$ and the inward flow along the y -direction are essential in balancing the vorticity stretching in the stationary solution which is called the Burgers vortex layer. The shear strength is measured by the x -direction velocity V_∞ far from the layer. The Reynolds number is naturally defined as $R = V_\infty/\sqrt{S\nu}$. For large Reynolds numbers the layer is destroyed by a Kelvin-Helmholtz-type instability. Linear stability analysis of the stationary case [3] shows stability below $R_{cr} = 1$.

The nonlinear evolution of growing disturbances leads toward saturated stable states of the vorticity field. Earlier studies [4, 5, 6] have concentrated on large wavelengths and arrays of vortex tubes. We have numerically computed the transition and the new stationary states after linear instability, for a range of wavelengths between a short-wave

cutoff (present in the linear stability theory as well) up to large enough lengths to see that in the limit the vorticity tends to separated Gaussian tubes, as predicted [5].

These vorticity configurations are of interest because the *only stable* ones under two-dimensional dynamics at a stagnation line are among them. This has been an expectation which we have now confirmed. We describe here the typical stretched vorticity field before any three-dimensional instabilities have set in. We use direct numerical simulation with several different kinds of initial conditions and perturbations.

We find that either a layer, or a periodic array of peaks (tubes) is stable for fixed Reynolds number *and fixed* spatial wavelength. A particular parameter range was found in which *both* configurations are stable to small perturbations. Depending on the two parameters, and on their configuration, various initial fields evolve toward a stable state, thereby displaying the creation, merger, depletion, or spreading of tubes into a layer. We discuss the direction and time-scales of these transitions.

2 Formulation

Nondimensional variables are defined by choosing the time-scale to be $1/S$ and the length-scale to be δ . The scalar vorticity equation is then written as

$$\frac{\partial \omega}{\partial t} + \left(\frac{\partial \omega}{\partial y} \frac{\partial}{\partial x} - \frac{\partial \omega}{\partial x} \frac{\partial}{\partial y} \right) \left(\frac{\partial^2}{\partial x^2} + \frac{\partial^2}{\partial y^2} \right)^{-1} \omega - y \frac{\partial \omega}{\partial y} = \omega + \left(\frac{\partial^2}{\partial x^2} + \frac{\partial^2}{\partial y^2} \right) \omega. \quad (1)$$

Fast spatial decay is required in the direction of compression y while periodicity is assumed in the x -direction. The Reynolds number is defined, in agreement with linear theory, by

$$R = \frac{1}{2L} \int_{-\infty}^{+\infty} dy \int_0^L dx \omega(x, y, t) \quad (2)$$

which is the nondimensional average shear and L is the nondimensional spatial period length. If the vorticity decays fast enough in the y -direction to be integrable for each fixed x , its integral over a period in x , and hence R , is time-independent. To distinguish different solutions obtained at same R and L , one uses time-dependent functionals, e.g. the maximum vorticity $\omega_{\infty}(t) = \max_{y,x} |\omega(y, x, t)|$.

For numerical integration we use an explicit fourth-order Runge-Kutta scheme to advance the solution in time, and spectral discretization of the spatial derivatives. The computational domain is rendered finite by truncation: $|y| < M$ defines a symmetrically placed strip around the x -axis. For $M \gg 1$ the finite-domain problem produces a localized vorticity field which in practice cannot be distinguished from the infinite strip solution. On the two artificial boundaries of the domain, both vorticity and streamfunction are required to vanish. This agrees with vorticity decay and assures there is no flow into the domain except for the stagnation flow. Fourier in x and sines in y . The nonlinear term and the linear inhomogeneous term in (1) are calculated in physical space. Dealiasing is made by the 2/3 rule.

3 Typical configurations: layers and tubes only

We used different kinds of initial conditions in order to find out which are the typical emerging coherent structures. For same R and L we used: (1) collections of circular or elliptic vortex tubes of varying strength, size, and initial position; (2) vorticity layers of different profiles, intensity, thickness, and initial displacement from the center line, their combinations or sinusoidal perturbations of amplitude or axis; (3) randomly generated vorticity distributions. These cases were forced only by the stagnation flow. Alternatively, we ran simulations starting *from zero vorticity* and evolving in the presence of a random forcing. We used centered white noise independently prescribed at each collocation point. This is no realistic model for the forcing that modulates vorticity close to actual flow stagnation points, but precisely because of this, it is expected that typical vorticity structures computed from this crude approximation will be the most robust.

The results from all simulations show that *vortex layers* and *chains of tubes* represent the only typical structures in a two-dimensional stagnation flow. All other features are fast transients; a layer and different tube arrays can transform into each other depending on the values of R and L but this requires usually a longer time.

3.1 Effect of initial condition

A series of simulations were started from initial states of uniform (or zero) vorticity over the computational domain, with added low-amplitude random initial perturbation. Vorticity is smoothed by viscosity and compressed by the stagnation flow *initially into a layer*. If the initial total vorticity is sufficiently large, roll-up follows; the resulting “tubes” depend on the random initial state, but merge finally into one, producing a stationary state.

The same qualitative picture was observed for smooth initial conditions. Instability of layers and merger of densely situated tubes have similar time-scales and leading to a single stationary “tube” per spatial period available. The opposite process when sets of tubes merge into a single layer, is observed as well, but the final phase, in which any vorticity peaks spread out, is very slow. This can be expected, since the process is not convective but due to viscous diffusion only.

3.2 Random forcing

The “Grasshof number” G is the noise dispersion integral divided by the area of the domain. In each separate run it is fixed by the time-independent noise intensity. The Reynolds number based on total vorticity is no longer constant. The average “vorticity” added by the noise over a short interval is small and vanishes in the time average.

It may seem that emerging coherent structures should have zero mean vorticity, e.g. a perturbed version of the Kerr and Dold solution [7] representing a chain of vortex tubes with alternating signs and equal strength. But we did not find stable configurations with small total vorticity. For low G the Reynolds numbers of the induced flow is low, as well. Regions of strong positive or negative vorticity do not survive for times longer than $O(1)$. Above some G_{cr} a randomly created vorticity concentration can be strong enough to survive. Our observations suggest that for this it is essential that the vorticity along the center line is of the same sign (as in a Burgers vortex layer) and strong enough (in fact, the observed layer is supercritical and rolls up). A vortex tube is thus created out of noise

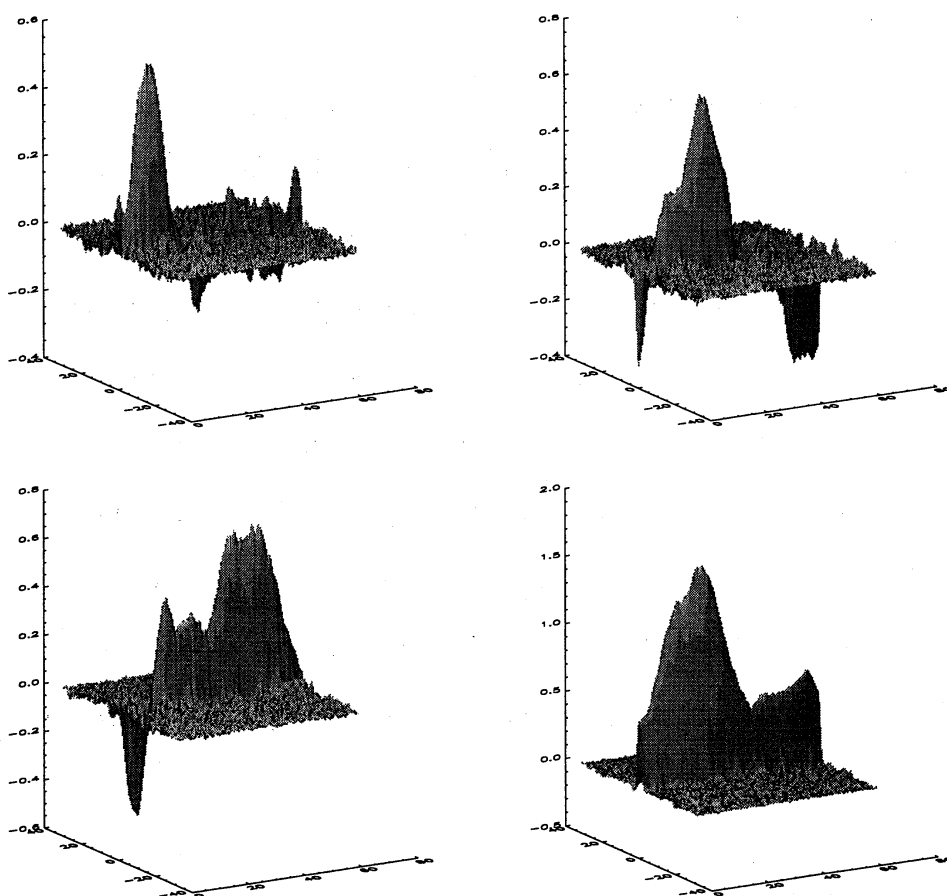


Figure 1: Randomly forced $-\omega(t)$ field, early times: 10 (upper left), 100 (upper right), 250 (lower left), 270: layer (lower right). The maximum vorticity amplitude at the center line remains about 0.5–0.6, except for the peak in the last frame which has a maximum about 2.0 and shows the initial growth of a tube-like structure.

with *zero average*, but not in all runs and only when the fluctuations are strong enough.

At early times of a particular run, the vorticity field shown in Fig. 1 distantly resembles various kinds of structures such as a layer (ridge), a single tube (peak), a couple of peaks with opposite sign, etc. until the time a “layer” is formed (all vorticity concentrated at the center line spontaneously assumes the same sign as shown in the last frame of Fig. 1). It can also be detected as a fast and strong increase in total vorticity. Subsequent formation of a tube is illustrated in Fig. 2. It can be detected as a fast increase in ω_∞ by orders of magnitude. The tube is strong enough to resist perturbations at later times.

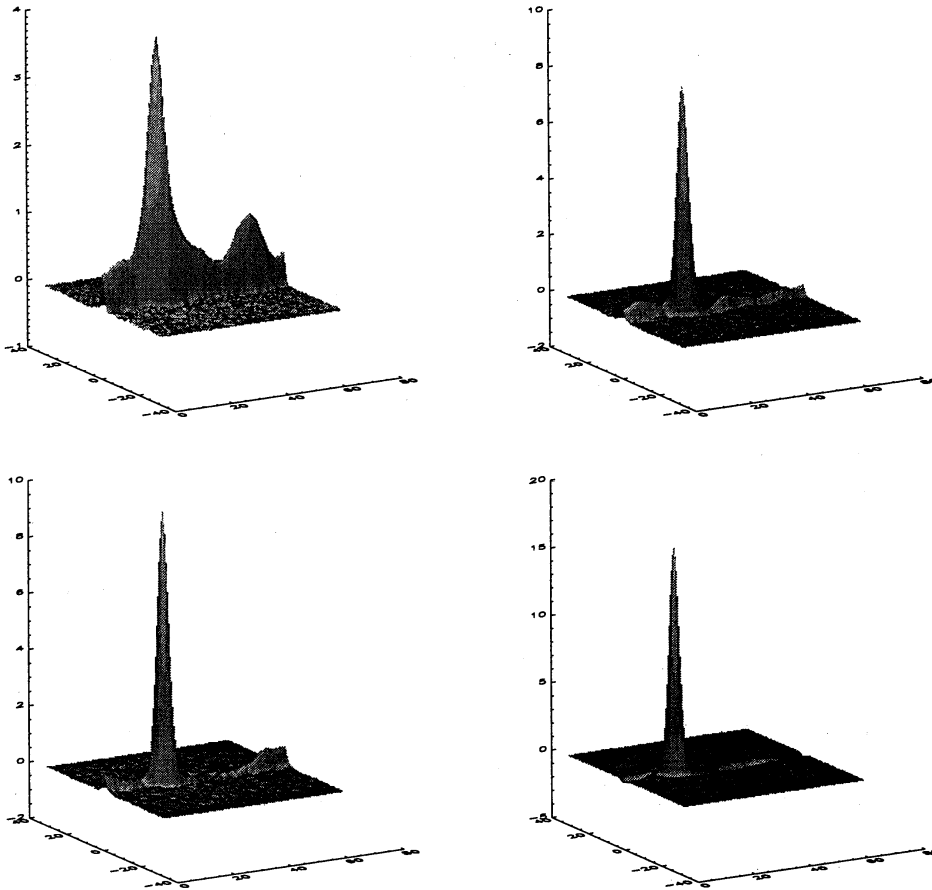


Figure 2: Randomly forced $-\omega(t)$ field, tube evolution at times: 320 (upper left), 360 (upper right), 400 (lower left), 500 (lower right). The vertical scale (vorticity amplitude) grows with time: fast during roll-up (approximately from 4 to 18 in the frames shown), slowly and fluctuating afterwards. The amplitude of the center line layer decreases.

4 Transitions between vorticity configurations

Given that layers and tubes are the dominant structures, we looked at their mutual transformations. Both transitions from tube-dominated configurations to layers and vice versa can take place, depending on the Reynolds number and the wavelength. Only mergers and no disintegration of tubes are observed.

The transition from layers to tubes can be predicted well from linear stability theory: It occurs only for strong layers, due to the existence of a critical Reynolds number [3]. There is a finding from the present simulations, however, which does not follow intuitively (although it is predictable, by way of a weakly nonlinear perturbation analysis) from the

linear theory: for $L \gg 1$, within a range $0 < R_0 \leq R < 1$ with $R_0(L)$ decreasing as L is increased, both the layer and the single tube are stable. Depending on initial condition, simulations produce both states.

4.1 Spread or roll-up: effect of Reynolds number and wavelength

In a supercritical perturbed vortex layer, instabilities develop initially at a time-scale given by the growth-rate of a Burgers vortex layer linear instability. The nonlinear growth phase, however, follows fast within an $O(1)$ time span. Subsequent saturation of the formed tubes shows linear decay rate. Linear growth fits for one case are shown in Fig. 3. Like in several other cases, we have computed the linear growth-rates and confirmed that they agree well (maximum error 1%) with good fits to the numerically computed dynamics of ω_∞ . Total enstrophy plots are similar to the ones for ω_∞ like Fig. 3. The fast growth coincides with the nonlinear process of concentration of vorticity.

A larger Reynolds number or a wavelength which is neither too large or too close to the cutoff length, make the time span of the transition much shorter by increasing linear growth-rates. A larger Reynolds number reduces the excentricity of resulting vortex cores.

Runs from initial conditions comprised of localized elliptic vortex tubes with Gaussian profiles of various amplitude, orientation, size, and location, have shown that tubes are first convected to the stagnation line. Once there, weak or diffuse tubes of like or opposite sign merge due to the viscous diffusion of vorticity in the x -direction. If the tubes are strong and localized, however, they merge into a single tube. When L is increased, the time-scales of both creation and spreading of tubes become large.

4.2 Merger of stretched tubes

When more than one tube is present in one spatial period, their merger is observed. Pairing and other subharmonic instabilities are well understood for inviscid periodic vortex arrays (see [8] and the references therein). Coalescence of both like and opposite sign vortices

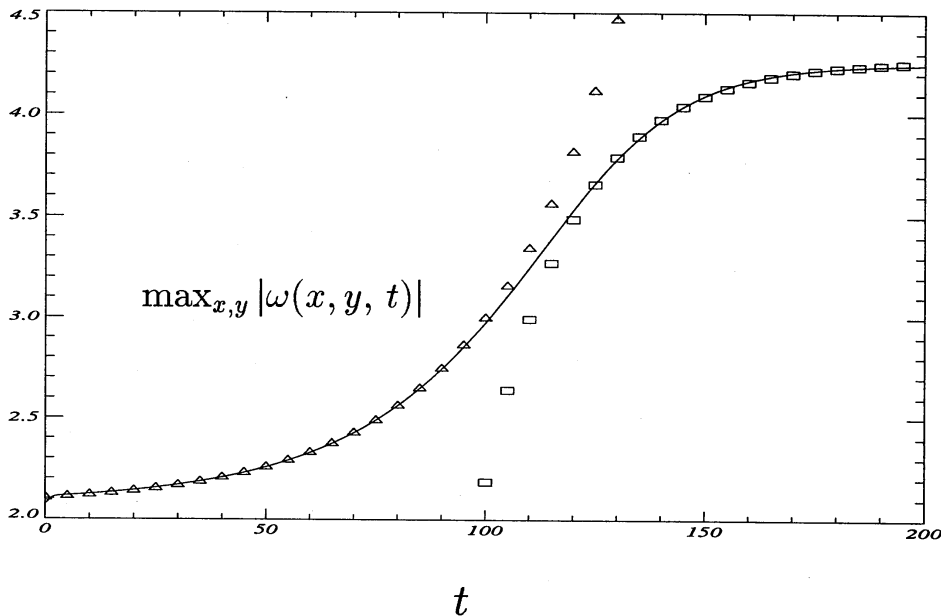


Figure 3: Exponential growth and saturation of the maximum vorticity. Solid line: numerical data of vorticity maxima of perturbed Burgers vortex layer, $R = 2.6$ and $L = 16$. Triangles: growth rate 0.0315, exponential fit. Squares: saturation rate -0.049 , exponential fit.

bears qualitative similarity to that in stagnation points with two axes of compression [9].

Merger of like-sign vortices develops in time similarly to the Burgers vortex layer instability: Slow phase of approach, fast nonlinear merger with sharp increase of enstrophy and maximum vorticity, and a linear saturation phase when the stronger single tube relaxes to a more circular shape. The typical graph of ω_∞ consists of several “jumps” similar to that in Fig. 3, which correspond to separate merger events.

In both roll-up or merger at high Reynolds numbers, transient states have spiral vorticity wrapped around the central core. The filaments are eventually diffused into a layer trace that connects the cores. It becomes more straight and decreases in amplitude very fast with the increasing R or L .

5 Concluding Remarks

Positive excess energy (above that of the Burgers vortex layer flow) and higher rate of energy dissipation of the tube solutions is perceived physically related to the layer and

merger instabilities. For $L \gg 1$ several stationary tube-like solutions exist, corresponding to the integer fractions of the spatial period, which remain above the short-wave cutoff. These are subject to subsequent merger due to a subharmonic instability. Viscous two-dimensional pairing instability is worth a separate study, including estimation of linear growth-rates. They should fall off fast when the spatial period of the basic flow is increased.

No other types of final states than stationary solutions were observed, neither other *stable* stationary solution branches. It seems that the two-dimensional dynamics has a simple attractor even at high Reynolds numbers, when fast spatial decay is required for the vorticity. The significance of this depends on the survival of the coherent structures considered here. Their three-dimensional stability has remained outside our present scope.

References

- [1] G. K. Batchelor (1967), *An Introduction to Fluid Dynamics*, Cambridge Univ. Press.
- [2] F. S. Sherman (1990), *Viscous Flow*, McGraw-Hill Book Co.
- [3] K. N. Beronov and S. Kida (1996), "Linear two-dimensional stability of a Burgers vortex layer," *Phys. Fluids* **8**, 1024.
- [4] S. J. Lin and G. M. Corcos (1984), "The mixing layer: deterministic models of a turbulent flow. Part 3: The effect of plane strain on the dynamics of streamwise vortices," *J. Fluid Mech.* **141**, 139.
- [5] J. C. Neu (1984), "The dynamics of stretched vortices," *J. Fluid Mech.* **143**, 253.
- [6] T. Passot, H. Politano, P. L. Sulem, J. R. Angilella, and M. Meneguzzi (1994), "Instability of strained vortex layers and vortex tube formation in homogeneous turbulence," *J. Fluid Mech.* **282**, 313.
- [7] O. Kerr and J. W. Dold (1994), "Periodic steady vortices in a stagnation-point flow," *J. Fluid Mech.* **276**, 307.
- [8] P. G. Saffman and R. Szeto (1981), "Stability and Structure of Stretched Vortices," *Stud. Appl. Math.* **65**, 223.
- [9] J. D. Buntine and D. I. Pullin (1989), "Merger and cancellation of strained vortices," *J. Fluid Mech.* **205**, 263.